The Force-Feedback Coupling Effect in Bilateral Tele-Impedance

Doornebosch, Luuk M.; Abbink, David A.; Peternel, Luka

DOI
10.1109/BioRob49111.2020.9224296

Publication date
2020

Document Version
Accepted author manuscript

Published in
Proceedings of the 8th IEEE RAS/EMBS International Conference for Biomedical Robotics and Biomechatronics, BioRob 2020

The Force-Feedback Coupling Effect in Bilateral Tele-Impedance

Luuk M. Doornebosch, David A. Abbink, and Luka Peternel

***Abstract*— In this paper, we introduce and explore a concept called *coupling effect*, which pertains to the influence of force feedback on the commanded stiffness that is voluntarily controlled by the operator through the stiffness interface during bilateral tele-impedance. The degree of coupling effect depends on the type of interface used to control the impedance of the remote robot. In case of muscle activity based stiffness command interfaces, the force feedback can invoke involuntary changes in the commanded stiffness due to human reflexes. These involuntary changes can be either beneficial (e.g., during position tracking) or detrimental (e.g., during force tracking) to the task performance on the remote robot side. To investigate the coupling effect in different types of stiffness command interfaces (i.e., coupled and decoupled), we conduct an experimental study in which participants are asked to perform position and force tracking tasks. The results show that in both position and force tracking tasks a lower tracking error of the reference stiffness is obtained with a decoupled interface ($p < 0.001$). However, the unexpected force perturbation yields lower absolute position error when using a coupled interface ($p = 0.0091$), which indicates a specific benefit of the coupling effect. Finally, a lower absolute force error is found in the force tracking task by using the decoupled interface ($p < 0.001$), which indicates a specific downside of the coupling effect.**

I. Introduction

Teleoperation is often applied when human-in-the-loop solution is preferred over automation (e.g., robot-assisted surgery, space robotics, transportation, etc.), or when automation is not capable to handle complex environmental interactions [1]. By using human-in-the-loop approach, the human operator's cognitive abilities can be incorporated into the remote robot so that it can efficiently deal with the uncertain and unpredictable interactions in unstructured environment [2]. Furthermore, teleoperation can be used for teaching the robot new interactive skills in an intuitive and online manner [3], [4].

Humans continuously interact with its unstructured and unpredictable surroundings in a very successful manner. The key to this is the ability of the central nervous system (CNS) to actively regulate the posture and mechanical properties of limbs [5], [6]. The endpoint viscoelastic properties of the limb are partly passive, but can also be adapted to a large extend due to co-contraction and reflexive activity. Co-contraction instantaneously changes the limb viscoelasticity, while reflexes induce muscle-activity that changes the viscoelastic properties and posture as a reflexive response to external forces acting on the limb [7]. This important human ability to regulate impedance is absent in classical tele-operation.

The authors are with Haptics Lab of Department of Cognitive Robotics, Delft University of Technology, Mekelweg 2, 2628 CD Delft, The Netherlands, e-mail: L.Peternel@tudelft.nl

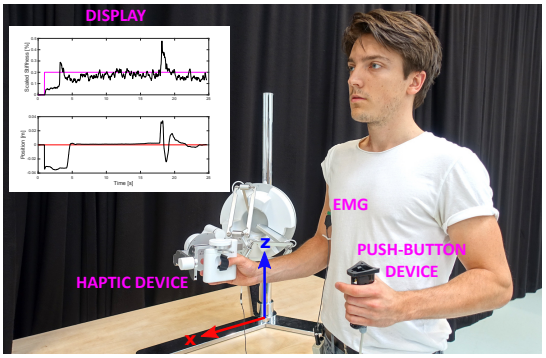

Fig. 1: Illustration of experimental setup. The Sigma.7 haptic device is controlled with the right arm. Two electrodes of the Delsys Bagnoli EMG-system are used. They are connected to the Bicep Brachii and the Tricep Brachii on the right arm. The push-button device is operated with the left hand. In the position tracking task the participant watched a display showing time traces of the commanded scaled stiffness and virtual slave position. A time trace of the virtual slave force was additionally provided in the force tracking task. Stiffness is commanded either with EMG measurements (coupled SCI) or the push-button device (decoupled SCI).

To equip the operator with the ability to actively regulate dynamic properties of the remote robot, a concept of tele-impedance was proposed in [8]. The concept was initially based on a unilateral teleoperation setup, where, besides sending position commands, the human could also map the estimation of their arm impedance to the remote robot impedance. This estimation was based on real-time electromyography (EMG) of relevant arm muscles and arm posture measurements. The additional impedance command channel allowed operators to perform better compared to fixed impedance for the studied experimental tasks. Unilateral tele-impedance provided a similar performance enhancement as seen in bilateral teleoperation, however, removed the associated stability issues [8]. Nonetheless, force feedback provides the human tele-operator with much better immersion into the remote environment [2], [9] and becomes crucial when visual feedback is not available [10], [11].

In literature, one generally finds three different types of methods for commanding real-time slave robot impedance that are applied to force-feedback teleoperation setups. The first method allows the operator command the impedance by the amount of grip force that is measured by the force sensor on the handle of the haptic interface [9], [12]. The second allows the operator to command the impedance by a hand-held external interface with a spring-return button [2], [13]. The third method employs real-time sEMG measurements of human arm to estimate human impedance and maps it to the remote robot [10], [11], [14].

In this paper, we investigate fundamental characteristics of different stiffness commanding interfaces (SCI) and intro-

duce a concept called *coupling effect*. We define it as a neuro-mechanical coupling between force feedback and human limb impedance that is used to command the remote robot's impedance. This coupling effect is particularly strong in SCI based on bio-signals like sEMG measurements [8], [11], [14] or electrical impedance tomography (EIT) [15], which we can categorise as coupled SCIs[1]. Since sEMG or EIT measure total muscle activity, the commanded impedance sent to the remote robot is a sum of voluntarily impedance changes and involuntarily impedance changes that can result from unexpected force feedback. On the other hand, we can categorise hand-held external devices [2], [13] as decoupled SCIs. In such case, involuntary changes in viscoelastic properties of operator's limb due to reflexes do not affect the commanded impedance, because there is no coupling effect between the force feedback and the stiffness commanding method.

Most of previous research in tele-impedance used coupled type slave impedance command interfaces [3], [8], [18]. However, since they mostly used a unilateral teleoperation setup, the coupling effect was not present. Whenever the concept of tele-impedance is used in a bilateral setup [2], [11]–[14], the coupling effect becomes important. When a human limb is unexpectedly perturbed, reflexes can cause an involuntary stiffening of the limb [7]. The same concept applies to bilateral tele-impedance; when a force feedback cannot be predicted, the human operator will involuntarily change its limb impedance to counter the perturbation due to reflexes.

In coupled SCIs that are based on sEMG measurements, when force feedback is present, the reflex stiffens up the arm in order to counter the unexpected force, which results in involuntarily increase of muscle activity. This hypothetically causes a temporal mismatch between the intended commanded slave stiffness, which is required to perform a given task and the actual commanded slave stiffness. While this temporal stiffness mismatch due to the coupling effect takes away some degree of operator's control over the remote robot impedance, it might not necessarily negatively affect the task performance on the robot side. For example, if the remote robot experiences undesired perturbations, the force feedback might make the human stabilise the remote robot naturally through the coupling effect.

Based on the above, we hypothesise that:

- *H1*: The force feedback negatively affects tracking of the desired commanded stiffness in a coupled-type of interface, while it has no effect in a decoupled type interface.
- *H2*: The coupling effect between force feedback and commanded stiffness helps a position tracking task in case of unexpected perturbations when using a coupled type of interface.
- *H3*: The coupling effect between force feedback and commanded stiffness negatively affects a force tracking task in case of physical interaction when using coupled type of interface.

To test these hypotheses we design an experiment consisting of two tasks: tracking position whilst getting a random perturbation, and establishing a contact with an unknown object. These tasks represent two fundamental types of interaction with unstructured environment, where adjusting the impedance is crucial. We tested two main experimental conditions (stiffness commanding with a coupled and decoupled interface) on these two tasks.

II. Methods

A. Theoretical examination of coupling effect

Fig. 2 illustrates a bilateral tele-impedance block scheme for the decoupled (left) and the coupled (right) condition. In the coupled condition, the commanded slave robot stiffness is a function of visual cues from the remote environment and force feedback. The visual cues determine the voluntary change in stiffness, while the force feedback can induce involuntary stiffness changes due to reflexes captured by the coupling effect. In the decoupled condition, the slave robot stiffness is solely determined by the operator's voluntary stiffness input based on visual cues from the remote environment.

In this study, the concept of coupling effect is analysed on a fundamental level in a controlled (clean) condition. Therefore we deliberately made the choice to avoid real-world bilateral teleoperation issues (i.e., delay, transparency, etc.), which could influence/corrupt the results of the coupling effect. To do so, we used a simulated impedance-controlled slave robot and remote environment that was generated on the same computer that was used for control of Sigma.7 haptic device. Nevertheless, delay and transparency issues in tele-impedance can be solved by the approach in [11].

It is also important to stress that our primary focus was on examining performance of the human operator on the remote robot side, since that is where the actual task exists. The focus is not on the effect of neuro-mechanical aspects on coupled SCI on the human operators side, as this dependency is a side effect from the interface design. Since decoupled SCI does not have such a side effect, the comparison can only be made by performance on the remote robot side.

We defined the control law for the coupled and decoupled interfaces as

$$\boldsymbol{F}_C = \boldsymbol{K}_h(\text{vol}, \text{ffb})(\boldsymbol{x}_d - \boldsymbol{x}_a) - \boldsymbol{D}\dot{\boldsymbol{x}}_a, \tag{1}$$

$$\boldsymbol{F}_D = \boldsymbol{K}_{device}(\text{vol})(\boldsymbol{x}_d - \boldsymbol{x}_a) - \boldsymbol{D}\dot{\boldsymbol{x}}_a, \tag{2}$$

where vectors $\boldsymbol{F}_C$ and $\boldsymbol{F}_D$ are the interaction forces at the slave (i.e., F_s in Fig. 2), acting from the robot on the environment, in coupled and decoupled scenario, respectively. Vector $\boldsymbol{x}_a$ is actual slave robot end-effector position and $\boldsymbol{x}_d$ is desired end-effector position, which comes from the human arm position x_{arm} (Fig. 2). Matrix $\boldsymbol{K}_h$ is the commanded stiffness in the coupled scenario, which is a function of voluntary (vol) operator commands and involuntary commands due to reflexes caused by the force feedback (ffb).

[1]Due to a strong correlation between the grip force and the arm stiffness [16], [17], interfaces based on grip force can be consider as coupled SCI.

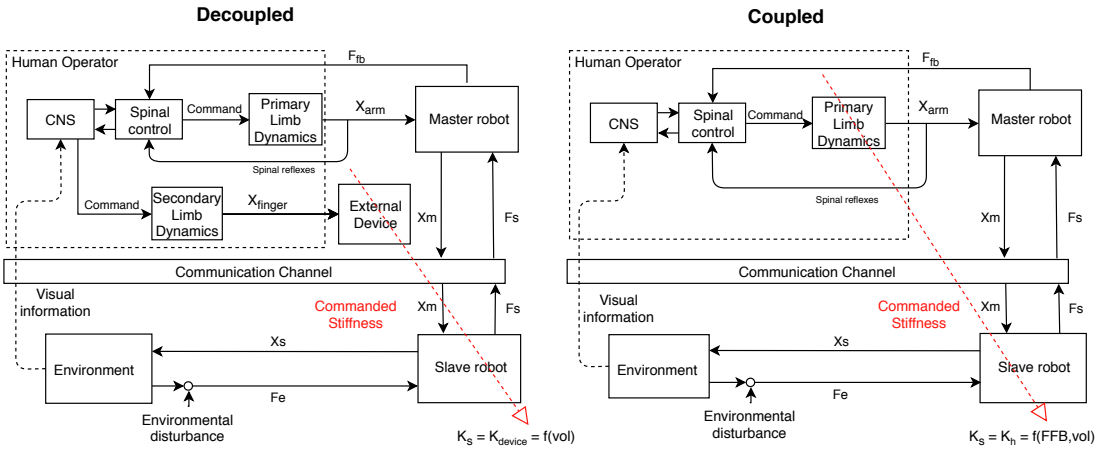

Fig. 2: A general scheme of a force-feedback tele-impedance setup is depicted for a decoupled SCI (left) and a coupled SCI (right). The primary limb refers to the limb holding the master robot. The secondary limb holds the external device in case of decoupled SCI. The human endpoint stiffness profile in the decoupled scenario is controlled by the finger position (x_{finger}) on an external device. Subscripts m, s and e correspond to master, slave and environment respectively. x, F and K correspond to position, force and stiffness respectively. The human arm stiffness profile is commanded to the slave robot through a communication channel. In case of coupled SCI, the human arm stiffness (K_h) is dependent on the voluntary muscle contraction due to visual information from the environment, as well as on reflexes induced by the force feedback (F_{fb}). In case of decoupled SCI, $K_h \neq K_s$ since $K_s = K_{device}$, which is manually commanded by the finger solely based on visual information from the environment.

Matrix $\boldsymbol{K}_{device}$ is the commanded stiffness through external device and is not influenced by reflexes. $\boldsymbol{K}_h$ and $\boldsymbol{K}_{device}$ are mapped to the slave stiffness $\boldsymbol{K}_s$ in each scenario, respectively. Damping matrix was defined as a function of the commanded stiffness matrix as $\boldsymbol{D} = 2\zeta\sqrt{\boldsymbol{K}}$, where damping coefficient ζ was set to 0.7 [19].

B. Experimental Setup

Sixteen participants (1 woman and 15 men) between 23 and 54 years old ($M = 25.9$, $SD = 7.5$) participated in the experiment. None of the participants had experience with teleoperation. Their participation was voluntarily and their efforts were not financially compensated for.

The experimental setup is shown in Fig. 1. We used a 7 degrees of freedom Force Dimension Sigma.7 haptic device to teleoperate a simulated remote robot. We examined translational movements in x-axis and constrained movements in the other axes. This means that the participant could only move the device forward and backward. Impedance control was implemented in both experimental tasks for both conditions (see (1) and (2)). A monitor was used to display actual and reference signals in real-time. In both tasks, reference stiffness and current commanded stiffness were displayed on one graph, while remote robot actual positions on the other graph. A graph which showed interaction force was additionally provided solely in the force tracking task. In the position tracking task, the reference was also displayed in the actual position graph. In the force tracking task, the reference contact force was also displayed in the actual force graph. Visual feedback about the perturbation (an object hitting the robot) in the remote environment was not provided in order to ensure the subject could not predict the impact.

For coupled SCI, we measured muscle activity by Delsys Bagnoli sEMG system. As in [18], we used Bicep Brachii and Tricep Brachii antagonistic muscle pair to estimate the human arm stiffness trend. We processed the measured sEMG signals in real-time: first 2nd order high-pass filter (cutoff 20 Hz), then rectification and finally 2nd order low-pass filter (cutoff 2 Hz).

We defined slave stiffness K_s for both coupled and decoupled SCI as

$$K_s = \alpha K_{max}, \tag{3}$$

where K_{max} is the maximum possible controllable slave stiffness, which is scaled by the interface control factor α.

In case of coupled SCI, we calculated it by

$$\alpha_c = K_h \cdot s_k, \tag{4}$$

where α_c is the coupled scaling factor that depends on the current stiffness trend estimation K_h. We use parameter s_k to select the muscle activation range used for the stiffness command. Since high co-contraction is very demanding and cannot be maintained for a longer period, the upper range is not practical for control of the remote robot stiffness. In our case, we set s_k to 0.5, which would correspond to 50% of co-contraction. Co-contraction estimation was calculated as

$$K_h = \frac{a_b + a_t}{2}, \tag{5}$$

where muscle activations a for Biceps and Triceps were obtained by normalising processed EMG signals to their maximal voluntary contraction (MVC) as

$$0 \leq a(t) = \frac{EMG(t)}{MVC} \leq 1. \tag{6}$$

In case of the decoupled SCI, we calculated the control factor α_d by

$$\alpha_d = \frac{V(x_{finger})}{V_{max}}, \tag{7}$$

where voltage V of potentiometer that depends on the current position of the spring-return button is normalised by the

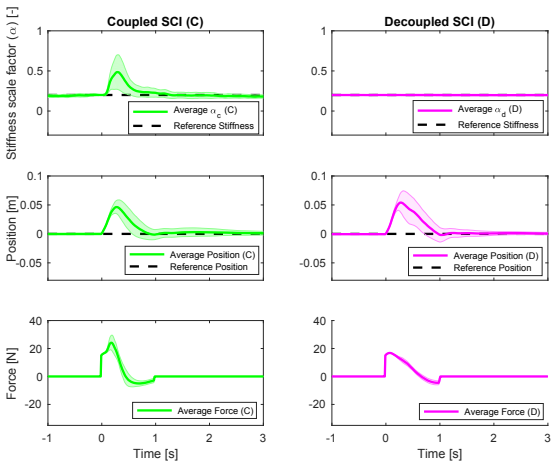

Fig. 3: The average over all 16 participants in the position tracking task is depicted within a four second time interval for coupled (left) and decoupled (right) SCI. A cloud of one standard deviation is plotted around the averaged data sets.

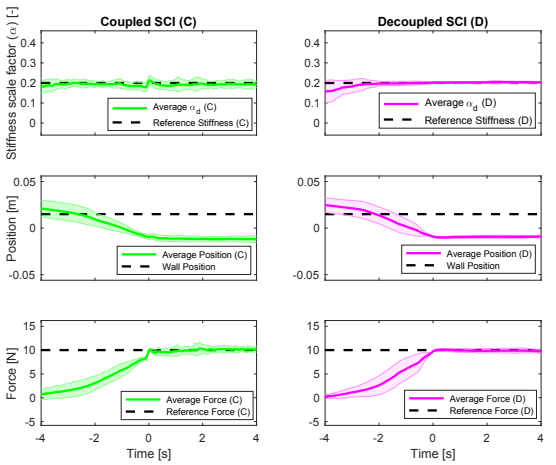

Fig. 4: The average over all 16 participants in the force tracking task is depicted within an eight second time interval for coupled (left) and decoupled (right) SCI. A cloud of one standard deviation is plotted around the averaged data sets.

maximum voltage V_{max}. From here on forward, the spring-return linear potentiometer used as decoupled SCI is called *push-button device*.

Both sEMG and push-button signals were sampled at 1000 Hz by a National Instruments DAQ device (USB-6002). These signals as well as the force and position measurements from Sigma.7 were processed in C++ and sent to Matlab/Simulink via UDP packages (local host) to be displayed to the participant in real-time plots.

C. Experimental protocol

Before the experiments, each participant performed MVC of the relevant muscles used in the experiments. During the experiments, the participants took a standing pose in front of the Sigma.7 master device. The height of the Sigma.7 was adjusted so that it was held comfortably at 90 degrees of elbow flexion (Fig. 1).

Each participant was first familiarised with the stiffness commanding methods during pre-trials, where a reference stiffness signal was followed using both SCIs. The reference stiffness signal in the familiarisation pre-trials was identical for both SCIs and consisted of four step functions and a chirp signal of two periods. The value ranged between 4% and 25% of the coupled and decoupled scaling factors: (4) and (7). To minimise the learning effects, participants performed additional training trials before every task. The training trial was similar to that of the task trial except that different representable dependent variables were chosen.

The experiment used a repeated measures design. Every participant was tested in two tasks with two different SCIs for five repetitions. The coupled SCI used the participant's sEMG measurements to command the slave robot stiffness and the decoupled SCI used the push-button device to command the slave robot stiffness. This resulted in four combinations of task and SCI. To keep the participants engaged and mitigate further practise effects, the order in which the participants received the conditions was randomised based on a balanced Latin Square. The tasks were defined as:

Position tracking: The participant was asked to move the Sigma.7 to the reference position and keep it there. When this reference position was reached, the participant tried to maintain the reference stiffness (through either coupled or decoupled SCI), while simultaneously keeping the reference position. The primary goal of the participant was to maintain this reference position as well as possible. After the force perturbation at a random time, the participant had to bring the robot back to reference position and command the correct stiffness according to the reference.

Force tracking: The participant was asked to move the Sigma.7 towards them (in front of the virtual wall). The virtual wall would appear after 15 seconds (for safety reasons). When the wall appeared, the participants were given a verbal conformation from the experimenter. When the participant comfortably maintained the reference stiffness, he/she approached the wall to establish contact and then tried to maintain the reference interaction force of 10N and reference stiffness simultaneously. The primary goal of the participant was to maintain this reference interaction force as well as possible.

The conditions for each task were defined as:

Perturbation: While the participant was tracking the position and the stiffness reference, a perturbation occurred at a random time. This perturbation force is equivalent to a mass of 5kg hitting the impedance-controlled virtual slave robot with a velocity of $1\frac{m}{s}$. Conservation of momentum principle was used to calculate the states of the slave robot and in turn the force feedback provided by the master device. The reference stiffness signal was set at 20% of the maximum virtual slave robot stiffness ($K_{max} = 500\ \frac{N}{m}$). This force perturbation lasted for one second.

Virtual wall: When the participant initiated forward movement while tracking the stiffness reference, the contact with the wall was established at $x = 0.015$m. The reference stiffness signal was set at 20% of the maximum virtual slave robot stiffness ($K_{max} = 2000\ \frac{N}{m}$). The force feedback due to

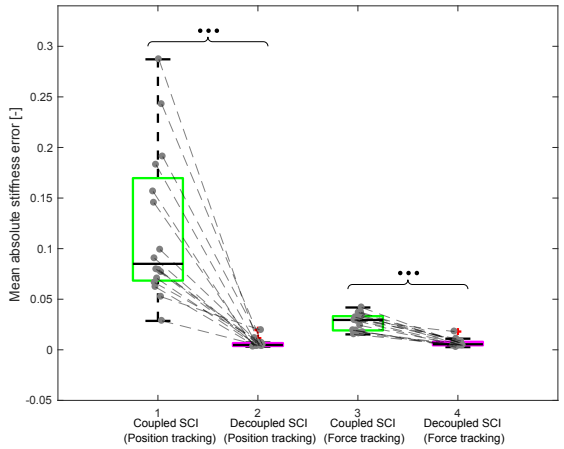

Fig. 5: Boxplots of the mean absolute error of the deviation from reference stiffness during the force perturbation in the position tracking task is depicted on the left. The mean absolute error of the deviation from the reference stiffness during 4 second of 10N pressing contact with the virtual wall (force tracking task) is depicted on the right. In the coupled SCI and the decoupled SCI every single participant is represented by a magenta dot. The within-subject difference is represented by the grey dotted lines connecting the dots. The black dots (●●●), (●●), (●) indicate a significance of $p \leq 0.001$, $p \leq 0.01$, $p \leq 0.05$.

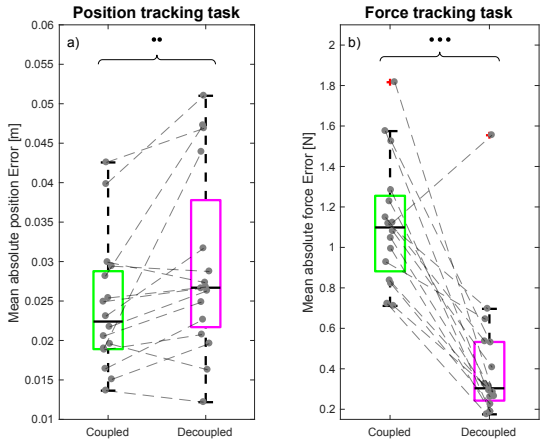

Fig. 6: a) Boxplots of the mean absolute error of the deviation from reference position during the force perturbation. b) Boxplots of the mean absolute error of the deviation from reference force during 4 second of 10N pressing contact with the virtual wall. In coupled SCI (left) and decoupled SCI (right), every single participant is represented by a magenta dot. The within-subject difference is represented by the grey dotted lines connecting the dots. The black dots (●●●), (●●), (●) indicate a significance of $p \leq 0.001$, $p \leq 0.01$, $p \leq 0.05$.

impedance control of slave was felt by the participant when the contact was established with the wall.

D. Data analysis

We analysed stiffness, position and force signals during the period of force feedback. To describe the participant's performance in tracking specific references, we used the following metric: average over the mean absolute error between signal and reference signal of the five repetitions. For statistical analysis we performed paired sample t-tests.

III. Results

Fig. 3 and Fig. 4 show the average results of all 16 participants for position tracking and force tracking, respectively. These figures provide an overview of the effect of force feedback on the commanded stiffness in different tasks. For more detailed insight, the coming paragraphs show results regarding the effect on commanded stiffness, position tracking and force tracking for different SCIs.

A. Coupling effect on commanded stiffness

In the position tracking and force tracking tasks, the commanded stiffness in coupled SCI is influenced by the two different force-feedback scenarios (perturbation and contact). Fig. 5 shows the mean absolute stiffness error in both tasks during the force feedback duration. The absolute mean commanded stiffness error in the position tracking task was higher when coupled SCI was used, compared to when decoupled SCI was used. The difference was statistically significant $t(15) = 9.66$, $p \leq 0.001$. The absolute mean commanded stiffness error in the force tracking task was higher when the coupled SCI was used, compared to when decoupled SCI was used. The difference was statistically significant $t(15) = 11.54$, $p \leq 0.001$. Fig. 3 and Fig. 4 show the scaled stiffness averaged over the participants, and the difference between using coupled SCI and decoupled SCI in both tasks is evident.

B. Coupling effect on position tracking

In the position tracking task the mean absolute error from the reference position during the force feedback was compared between the two SCIs. The mean absolute position error in the position tracking task was higher when the decoupled SCI was used, compared to when coupled SCI was used. The difference was statistically significant $t(15) = -2.97$, $p = 0.0096$. This is depicted in Fig. 6 a). Fig. 3 shows this difference between coupled SCI and decoupled SCI for the position tracking task in the position graph.

C. Coupling effect on force tracking

In the force tracking task the mean absolute error from the reference force during 4 second, 10N pressing contact with the virtual wall was determined. The mean absolute force error in the force tracking task was higher when the coupled SCI was used, compared to when decoupled SCI was used. The difference was statistically significantly $t(15) = 7.45$, $p \leq 0.001$. This is depicted in Fig. 6 b). Fig. 4 shows this difference between coupled SCI and decoupled SCI for the force tracking task in the force graph.

IV. Discussion

Due to the coupling effect, the commanded stiffness in both the position tracking task and the force tracking task was negatively affected by the force feedback in the coupled SCI. This occurred because the force feedback triggered reflexes that involuntarily changed the commanded stiffness away from the desired reference stiffness. These results are in line with our first hypothesis *H1*.

The coupled SCI allowed for better position tracking, compared to using the decoupled SCI, when a force perturbation disturbed the operator unexpectedly through force feedback. This is due to the coupling effect, where human reflexes can be exploited to help counteract the perturbation, since the operator's arm naturally stiffens up. Involuntary stiffening of the arm is a result of a rapid muscle activity increase, which also yields a higher commanded stiffness to the remote robot. Increasing the commanded stiffness with this speed cannot be reached with the decoupled SCI because voluntary actions are slower compared to reflexes. The increased stiffness of the remote robot makes the position tracking stricter according to the impedance control law and improves the task performance. These results are in line with our second hypothesis *H2*.

The decoupled SCI allowed for better force tracking compared to using the coupled SCI when producing a reference force on an external object. The coupling effect adversely influences the ability to maintain a stable contact. The contact produced fluctuations in force feedback, which can be perceived as small force perturbations. Due to the coupling effect, this induces involuntary stiffness changes through the operator's reflexes. These results are in line with our third hypothesis *H3*.

We should note that sEMG based interfaces are not necessary intended to keep some reference stiffness, since the operator can naturally perform the task in accordance to the environmental interaction. If dynamics of the human arm and the robot arm are comparable, using coupled SCI can be intuitive and the coupling effect can be used as a natural aid. This can be especially beneficial in presence of random perturbation, and when visual feedback is limited or unavailable. However, if dynamics of slave and master are drastically different (e.g., operating a heavy-load robot or operating a microscopic surgical robot), the coupling effect may produce unnatural reactions detrimental to the task. When the scaling of dynamics is not comparable, the decoupled SCI might be preferred over the coupled SCI.

We should stress that this study was performed in absence of common real-world bilateral teleoperation issues (i.e., delay, transparency, etc.) in order to obtain uncorrupted results and examine the coupling effect on a fundamental level. This kind of a controlled (clean) study can serve as a baseline for future studies of influences of specific bilateral teleoperation issues on the coupling effect.

These novel fundamental insights in the coupling effect during bilateral tele-impedance should be an important consideration for users and applications. They highlight tradeoffs that can help to select the right stiffness interface for the given use-case. Furthermore, they create awareness about a possible mismatch between commanded stiffness and desired stiffness due to the coupling effect, which does not necessarily have a deleterious effect on task performance. As a general guideline, we recommend to use coupled SCI for tasks which require accurate tracking or maintaining of robot position, and decoupled SCI for scenarios where the robot should establish a contact or maintain a constant force.

REFERENCES

[1] H. Boessenkool, D. A. Abbink, C. J. Heemskerk, F. C. van der Helm, and J. G. Wildenbeest, "A task-specific analysis of the benefit of haptic shared control during telemanipulation," *IEEE Transactions on Haptics*, vol. 6, no. 1, pp. 2–12, 2012.

[2] L. Peternel, T. Petrič, and J. Babič, "Robotic assembly solution by human-in-the-loop teaching method based on real-time stiffness modulation," *Autonomous Robots*, vol. 42, no. 1, pp. 1–17, 2018.

[3] L. Peternel, T. Petrič, E. Oztop, and J. Babič, "Teaching robots to cooperate with humans in dynamic manipulation tasks based on multi-modal human-in-the-loop approach," *Autonomous robots*, vol. 36, no. 1-2, pp. 123–136, 2014.

[4] L. Peternel, E. Oztop, and J. Babič, "A shared control method for online human-in-the-loop robot learning based on locally weighted regression," in *2016 IEEE/RSJ International Conference on Intelligent Robots and Systems (IROS)*. IEEE, 2016, pp. 3900–3906.

[5] N. Hogan, "Adaptive control of mechanical impedance by coactivation of antagonist muscles," *IEEE Transactions on automatic control*, vol. 29, no. 8, pp. 681–690, 1984.

[6] E. Burdet, R. Osu, D. W. Franklin, T. E. Milner, and M. Kawato, "The central nervous system stabilizes unstable dynamics by learning optimal impedance," *Nature*, vol. 414, no. 6862, p. 446, 2001.

[7] D. A. Abbink, M. Mulder, F. C. Van der Helm, M. Mulder, and E. R. Boer, "Measuring neuromuscular control dynamics during car following with continuous haptic feedback," *IEEE Transactions on Systems, Man, and Cybernetics, Part B (Cybernetics)*, vol. 41, no. 5, pp. 1239–1249, 2011.

[8] A. Ajoudani, N. Tsagarakis, and A. Bicchi, "Tele-impedance: Teleoperation with impedance regulation using a body–machine interface," *The International Journal of Robotics Research*, vol. 31, no. 13, pp. 1642–1656, 2012.

[9] D. S. Walker, "Design of versatile telerobotic systems using variable impedance actuation and control," Ph.D. dissertation, Stanford University, 2013.

[10] M. Laghi, A. Ajoudani, M. Catalano, and A. Bicchi, "Tele-impedance with force feedback under communication time delay," in *2017 IEEE/RSJ International Conference on Intelligent Robots and Systems (IROS)*. IEEE, 2017, pp. 2564–2571.

[11] M. Laghi, A. Ajoudani, M. G. Catalano, and A. Bicchi, "Unifying bilateral teleoperation and tele-impedance for enhanced user experience," *The International Journal of Robotics Research*, vol. 39, no. 4, pp. 514–539, 2020.

[12] D. S. Walker, R. P. Wilson, and G. Niemeyer, "User-controlled variable impedance teleoperation," in *2010 IEEE International Conference on Robotics and Automation*. IEEE, 2010, pp. 5352–5357.

[13] L. Peternel, T. Petrič, and J. Babič, "Human-in-the-loop approach for teaching robot assembly tasks using impedance control interface," in *2015 IEEE international conference on robotics and automation (ICRA)*. IEEE, 2015, pp. 1497–1502.

[14] C. Yang, C. Zeng, P. Liang, Z. Li, R. Li, and C. Su, "Interface design of a physical humanrobot interaction system for human impedance adaptive skill transfer," *IEEE Transactions on Automation Science and Engineering*, vol. 15, no. 1, pp. 329–340, Jan 2018.

[15] E. Zheng, Y. Li, Q. Wang, and H. Qiao, "Toward a human-machine interface based on electrical impedance tomography for robotic manipulator control," in *Intelligent Robots and Systems (IROS), 2019 IEEE/RSJ Intl. Conf. on*, Nov 2019, pp. 2768–2774.

[16] H. Nakamura, D. Abbink, and M. Mulder, "Is grip strength related to neuromuscular admittance during steering wheel control?" in *2011 IEEE International Conference on Systems, Man, and Cybernetics*, 2011, pp. 1658–1663.

[17] A. Takagi, G. Xiong, H. Kambara, and Y. Koike, "Endpoint stiffness magnitude increases linearly with a stronger power grasp," *Scientific Reports*, vol. 10, no. 1, pp. 1–9, 2020.

[18] A. Ajoudani, C. Fang, N. G. Tsagarakis, and A. Bicchi, "A reduced-complexity description of arm endpoint stiffness with applications to teleimpedance control," in *2015 IEEE/RSJ International Conference on Intelligent Robots and Systems (IROS)*. IEEE, 2015, pp. 1017–1023.

[19] A. Albu-Schaffer, C. Ott, U. Frese, and G. Hirzinger, "Cartesian impedance control of redundant robots: Recent results with the dlr-light-weight-arms," in *2003 IEEE International Conference on Robotics and Automation*, vol. 3. IEEE, 2003, pp. 3704–3709.